JOURNAL OF VIROLOGY, Dec. 2004, p. 13553–13561 Vol. 78, No. 24
0022-538X/04/$08.00+0 DOI: 10.1128/JVI.78.24.13553–13561.2004

In Vitro Characterization of a Simian Immunodeficiency Virus-Human Immunodeficiency Virus (HIV) Chimera Expressing HIV Type 1 Reverse Transcriptase To Study Antiviral Resistance in Pigtail Macaques

Zandrea Ambrose, Valerie Boltz, Sarah Palmer, John M. Coffin, Stephen H. Hughes, and Vineet N. KewalRamani*

HIV Drug Resistance Program, National Cancer Institute, Frederick, Maryland

Received 3 February 2004/Accepted 3 August 2004

Antiviral resistance is a significant obstacle in the treatment of human immunodeficiency virus type 1 (HIV-1)-infected individuals. Because nonnucleoside reverse transcriptase inhibitors (NNRTIs) specifically target HIV-1 reverse transcriptase (RT) and do not effectively inhibit simian immunodeficiency virus (SIV) RT, the development of animal models to study the evolution of antiviral resistance has been problematic. To facilitate in vivo studies of NNRTI resistance, we examined whether a SIV that causes immunopathogenesis in pigtail macaques could be made sensitive to NNRTIs. Two simian-human immunodeficiency viruses (SHIVs) were derived from the genetic background of SIV_{mne}: SIV-RT-YY contains RT substitutions intended to confer NNRTI susceptibility (V181Y and L188Y), and RT-$SHIV_{mne}$ contains the entire HIV-1 RT coding region. Both mutant viruses grew to high titers in vitro but had reduced fitness relative to wild-type SIV_{mne}. Although the HIV-1 RT was properly processed into p66 and p51 subunits in RT-$SHIV_{mne}$ particles, the RT-$SHIV_{mne}$ virions had lower levels of RT per viral genomic RNA than HIV-1. Correspondingly, there was decreased RT activity in RT-$SHIV_{mne}$ and SIV-RT-YY particles. HIV-1 and RT-$SHIV_{mne}$ were similarly susceptible to the NNRTIs efavirenz, nevirapine, and UC781. However, SIV-RT-YY was less sensitive to NNRTIs than HIV-1 or RT-$SHIV_{mne}$. Classical NNRTI resistance mutations were selected in RT-$SHIV_{mne}$ after in vitro drug treatment and were monitored in a sensitive allele-specific real-time RT-PCR assay. Collectively, these results indicate that RT-$SHIV_{mne}$ may be a useful model in macaques for the preclinical evaluation of NNRTIs and for studies of the development of drug resistance in vivo.

Reverse transcriptase (RT) is the viral enzyme targeted by many of the Food and Drug Administration (FDA)-approved drugs used to treat human immunodeficiency virus type 1 (HIV-1)-infected individuals. There are two types of reverse transcription inhibitors: nucleoside analogues (NRTIs) and nonnucleoside inhibitors (NNRTIs). NRTIs, which lack the 3′ OH found on normal nucleosides, inhibit reverse transcription by being incorporated by RT, prematurely terminating the viral DNA chain. NNRTIs are noncompetitive inhibitors that bind to RT, inhibiting the chemical step of DNA synthesis (35, 45). Most current antiviral therapy regimens include two NRTIs in combination with an NNRTI or a protease inhibitor (47).

Prolonged use of RT inhibitors may lead to the appearance of resistant virus. Common mutations leading to NNRTI resistance include K103N, Y181C, and Y188C (40), which contribute to the failure of NNRTI-containing regimens. In a study of a cohort of North American HIV-infected patients, the prevalence of transmitted NNRTI-resistant viruses increased from 1.9% during 1995 to 1998 to 7.1% in 1999 to 2000 (25). Similarly, genotypes of over 60,000 clinical isolates obtained worldwide between 1998 and 2002 were analyzed for HIV-1 drug resistance mutations (L. Bacheler, H. Vermeiren, P. McKenna, M. Van Houtte, and P. Lecocq, Abstr. 12th Int. HIV Drug Resist. Wkshp., abstr. 118, 2003), and the largest increase in resistance mutations over time in these samples was in those associated with NNRTI resistance. Eighty-three percent of NNRTI-resistant isolates were resistant to all three FDA-approved NNRTIs: delavirdine, efavirenz (EFV), and nevirapine (NVP). The development of NNRTIs that are effective against the common NNRTI-resistant strains is necessary for improved therapeutic options, including salvage therapy for HIV-infected individuals who have exhausted all of the available approved drugs.

Animal models to study HIV-1 antiviral resistance offer a number of advantages over in vitro culture systems. Studies in an appropriate animal model would better recapitulate features unique to viral replication in humans, including the presence of different subsets of primary cells susceptible to virus, immune selection pressure, and anatomically or immunologically privileged sites of replication, each of which could affect the evolution of antiviral resistance and/or the fitness of resistant isolates. Experimental infection of pigtail macaques (*Macaca nemestrina*) with SIV_{mne} provides a well-characterized model for AIDS pathogenesis and an alternative to the rhesus macaque (*Macaca mullata*), which are currently in short supply at U.S. primate centers (30). Moreover, SIV_{mne} isolates have also been reported to efficiently replicate in rhesus and cynomolgus (*Macaca fascicularis*) macaques (6, 7, 29, 36).

The RT protein of HIV-1 is approximately 60% identical to HIV-2 (42) and simian immunodeficiency virus (SIV) (18) RT molecules. Because of these differences, NNRTIs selected to target HIV-1 RT do not effectively inhibit the RT of HIV-2 or SIV, precluding the use of SIV-infected macaques for in vivo studies of NNRTI resistance. Two approaches have been employed to develop SIV with increased sensitivity to NNRTIs.

* Corresponding author. Mailing address: NCI—Frederick, Building 535, Room 108, Frederick, MD 21702-1201. Phone: (301) 846-5487. Fax: (301) 846-6777. E-mail: vineet@ncifcrf.gov.

One approach has been to make limited changes in the SIV RT sequence designed to minimize disruption of enzymatic activity. HIV-1 RT comprises five distinct structural elements, and active chimeras have been obtained by swapping these regions between HIV-1 and HIV-2 (42). Selective mutation of RT residues between 176 and 190 of HIV-2 (43) or SIV_{mac239} (18) has been used to generate viruses with increased sensitivity to NVP and TIBO R82913, an experimental NNRTI. However, chimeric viruses that contain partial HIV-1 RT sequences are not as susceptible to these NNRTIs as HIV-1. To date, no SIV-based chimeric virus has been evaluated with the second-generation FDA-approved NNRTI EFV.

A more successful strategy has been to replace the entire SIV_{mac239} RT with $HIV\text{-}1_{HXB2}$ RT (RT-$SHIV_{mac239}$) (5, 46). RT-$SHIV_{mac239}$ is as sensitive to NNRTIs as HIV-1. However, replication of RT-$SHIV_{mac239}$ is significantly impaired in vitro relative to wild-type SIV_{mac239} (44, 46). This impaired replication is partially relieved by mutating the suboptimal tRNA-Lys3 primer binding site (PBS) present in wild-type SIV_{mac239} to the canonical sequence present in HIV-1 (44). The relative fitness of RT-$SHIV_{mac239}$ with a modified PBS has not been formally compared to that of wild-type SIV_{mac239}, and it is unclear whether further changes would enhance the replication of RT-$SHIV_{mac239}$. Nonetheless, RT-$SHIV_{mac239}$ is able to maintain a persistent infection in rhesus macaques (37). Given its derivation from SIV_{mac239}, RT-$SHIV_{mac239}$ would be predicted to be restricted to the $CD4^+$ T-cell compartment for replication in vivo (26, 27).

Using a molecular clone of SIV_{mne}, we are developing a pigtail macaque model to study the effects of NNRTI therapy on HIV-1 RT and the relative fitness of drug-resistant viral isolates. SIV_{mne} achieves peak and persistent viremia comparable to that of SIV_{mac239} in vivo (20, 21, 38, 39), and SIV_{mne} encodes an optimal tRNA-Lys3 PBS. Prior studies with this isolate have indicated that it infects primary $CD4^+$ T lymphocytes and monocytes/macrophages (20), a subpopulation of cells that would be an important target for antiviral therapy. Here we describe an RT-SHIV derived from SIV_{mne} that is susceptible to first- and second-generation NNRTIs, replicates to high levels in cell culture, and upon in vitro selection develops NNRTI resistance mutations typically observed in drug-treated HIV-1 patients. We also describe a real-time RT-PCR assay that can be used to sensitively monitor the appearance and evolution of drug-resistant RT-$SHIV_{mne}$ isolates in vivo.

MATERIALS AND METHODS

Viral DNA. RT-$SHIV_{mne}$ was made by moving the RT coding region of $HIV\text{-}1_{HXB2}$ from the 5′ half of RT-$SHIV_{mac239}$, a kind gift from K. Überla (46), into the 5′ half of SIV_{mne} clone 8, a kind gift from G. Heidecker (13), using unique BamHI and SacI sites in each vector. SIV-RT-YY was made by PCR mutagenesis of the RT coding region of SIV_{mne} clone 8 at positions encoding amino acids 181 (V to Y) and 188 (L to Y). Overlapping sequences of the SIV_{mne} RT coding region containing the two mutations were obtained by PCR using the following primers: 5′-AATCCAGATGTGACCTTATACCAGTATATGGATG ACATCTACGTAGCT-3′ (inner) and 5′-TTCCTCCTATACCTTTGTGTGCT GGC-3′ (outer); 5′-TGTCCTGTCACTAGCTACGTAGATGTCATCCATAT ACTGGTATAAGGT-3′ (inner) and 5′-ACCAGTAGGCAACATTTACAGG AGATGG-3′ (outer). The 5′ half of SIV_{mne} clone 8 was used as the template. The reaction conditions were 94°C for 4 min; 5 cycles of 94°C for 1 min, 55°C for 1 min, and 70°C for 3 min; 25 cycles of 94°C for 1 min, 60°C for 1 min, and 70°C for 3 min; and 72°C for 7 min. The mutations introduced a unique SnaBI restriction site in the overlapping region of the PCR products. Each product was cloned into the pCR2.1 vector (Invitrogen, Carlsbad, Calif.). Each of the cloned RT sequences was then cleaved with SnaBI and subsequently ligated together. The ligated product and the 5′ SIV_{mne} clone 8 vector were digested with BamHI and HpaI and ligated together. The mutations encoding tyrosine residues were verified by DNA sequencing.

Cell culture medium. Cells were cultured in RPMI 1640 or Dulbecco's modified Eagle's medium (Invitrogen) containing 10% fetal bovine serum (Atlanta Biologicals, Norcross, Ga.), 100 U of penicillin/ml, 100 μg of streptomycin/ml, and 0.3 mg of L-glutamine (Invitrogen)/ml. RPMI was used for CEMx174 cells, and Dulbecco's modified Eagle's medium was used for 293T, JC53 BL13+, and sMAGI cells. Cells were incubated at 37°C in 5% CO_2.

RT inhibitors. In vitro RT inhibition assays were performed with zidovudine (AZT; Sigma, St. Louis, Mo.), didanosine (ddI; Sigma), stavudine (d4T; Sigma), lamivudine (3TC; Moravek, Brea, Calif.), tenofovir (NIH AIDS Reference and Reagent Program, Rockville, Md.), EFV (NIH AIDS Reference and Reagent Program), NVP (NIH AIDS Reference and Reagent Program), and UC781 (a kind gift from M. Parniak).

Virus replication kinetics. SIV_{mne}, RT-$SHIV_{mne}$, and SIV-RT-YY viral stocks were made by coprecipitation of 20 μg each of the 5′ and 3′ halves of each of the three proviral constructs after digestion with SacI, followed by electroporation into CEMx174 cells and passage for up to 6 weeks. Aliquots of each of the cultures were frozen at −80°C and analyzed for p27 production by SIV enzyme-linked immunosorbent assay (ELISA; Beckman Coulter, Miami, Fla.). $HIV\text{-}1_{NFN\text{-}SX}$ (31) and $HIV\text{-}1_{LAI}$ (23) stocks were generated by transfecting 293T cells with plasmid DNA by using the mammalian transfection kit (Stratagene, La Jolla, Calif.). Viral stock titers were determined on JC53 BL13+ indicator cells, a kind gift from J. Kappes (12). The in vitro infection and staining for β-galactosidase were performed as described previously (22). Briefly, indicator cells were plated at 2×10^4 cells/well in a 24-well plate. Virus was added to the cells in the presence of 10 μg of DEAE-dextran/ml and incubated for 2 h at 37°C. Cells were washed with sterile phosphate-buffered saline, followed by the addition of new medium and incubation for 48 h. Cells were fixed with 0.2% glutaraldehyde and 1% formaldehyde in phosphate-buffered saline for 5 min, washed in phosphate-buffered saline, and stained with 10 μg of 5-bromo-4-chloro-3-indolyl-β-D-galactopyranoside (X-Gal)/ml. Blue cells were counted on an inverted microscope.

Infections of CEMx174 cells with SIV_{mne}, RT-$SHIV_{mne}$, and SIV-RT-YY were performed at a multiplicity of infection (MOI) of 0.02 in the presence of 10 μg of Polybrene/ml for 2 h at 37°C. Infected cells were placed in medium in T25 flasks and incubated for 10 days. Aliquots were analyzed for p27 production by ELISA (Coulter Immunotech).

Viral sequencing. RNA was extracted from viral supernatants by using the RNeasy kit (QIAGEN, Valencia, Calif.). RT-PCR was performed using SuperScript one-step RT-PCR (Invitrogen) with primers (see below) and the following conditions: one cycle of 55 to 58°C for 30 min and 94°C for 2 min; 35 cycles of 94°C for 30 s, 58 to 60°C for 30 s, and 70°C for 2 min; and one cycle of 72°C for 10 min. Primers used for RT-PCR were the following: 5′-GCAAAAGGATTA AAGGGACAAT-3′ and 5′-GGGTAATCCAAATTTGAATACCAATTCT-3′ (RT); 5′-TGAAAGAGGCCCTTGCACC-3′ and 5′-ACAGGCTCTACCTTAG CTATGG-3′ (SIV-RT-YY NC); 5′-TGAAAGAGGCCCTCGCACC-3′ and 5′-ACAGGCTCTACTTTAGCTATGG-3′ (RT-$SHIV_{mne}$ NC); 5′-GCTAACAGC TCTGGAGATGTC-3′ and 5′-CATCCGACCTTATGATGG-3′ (SIV-RT-YY IN); 5′-GCTAACAGCTCTGGGGATGTC-3′ and 5′-TGCAGGTCCACCATG CC-3′ (RT-$SHIV_{mne}$ IN); and 5′-CGAGAAGTCCTCAGGACTGA-3′ and 5′-TCCTGGTCCCGAGGTGTAA-3′ (long terminal repeat polypurine tract [PPT]).

PCR products were either sequenced directly or TA cloned into the pcDNA3.1/V5-His Topo vector (Invitrogen). Multiple clones were picked and sequenced. Sequencing reactions were performed at the Laboratory of Molecular Technology (National Cancer Institute—Frederick) and Biotech Core (Mountain View, Calif.). Primers used for sequencing were the following: 5′-TAATACGACTCACTATAG GG-3′ (T7 in Topo vector); 5′-TAGAAGGCACAGTCGAGG-3′ (BGH reverse in Topo vector); 5′-GCTAACAGCTCTGGAGATGTC-3′; 5′-TGGAAGGGGTCA CCAGCCATCTTCCA-3′; 5′-TGGAAAGGATCACCAGCAATATTCCA-3′; 5′-GTGCTGGCTCTATCTTTTCCAAGAA-3′ (RT); and 5′-AGATAATGACTTG GTAGG-3′ (PPT).

Viral RNA quantitation. $HIV\text{-}1_{LAI}$ and RT-$SHIV_{mne}$ from cell culture supernatants were sedimented through a 20% sucrose cushion at 26,000 rpm at 4°C for 2 h in an AH629 rotor (Sorvall, Newtown, Conn.). Each sample was resuspended in RPMI. Viral RNA was quantified by reverse transcription and real-time PCR amplification, with an amplicon in HIV-1 *pol*. Viral RNA was isolated from 5, 2, and 1 μl of each sample by a guanidinium-isothiocyanate extraction method, as described previously (33). Briefly, a 190-bp amplicon in HIV-1 *pol* was converted to cDNA and amplified by real-time PCR by using gene-specific primers in a one-step RT-PCR. The total synthesized DNA was quantified using SYBR green fluorescence and compared to an RNA standard curve made from HIV-1 RNA transcripts. To minimize the contribution of nonspecific amplification to the fluorescent signal,

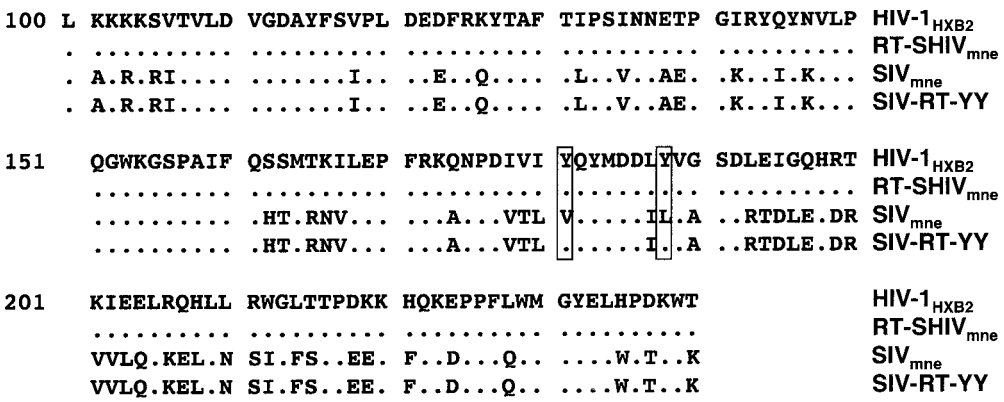

FIG. 1. Sequence alignment of amino acids 101 to 240 in the RTs of HIV-1_{HXB2}, RT-$SHIV_{mne}$, SIV_{mne}, and SIV-RT-YY. Dots indicate residues conserved between the different isolates. Boxed residues indicate residues 181 and 188, which are the residues that were changed to tyrosines in SIV-RT-YY.

fluorescence was measured at a temperature just below the melting temperature (T_m) of the correct product but above the T_m of nonspecific products. Additionally, a melting curve analysis of the RT-PCR products was routinely performed to confirm amplification specificity. All reactions were performed in an Opticon real-time PCR machine (MJ Research, Waltham, Mass.).

Western blot analysis. Recombinant HIV-1 RT protein (a kind gift from P. Boyer) and sucrose cushion-isolated HIV-1 and RT-$SHIV_{mne}$ were solubilized and run on a 4-to-12% gradient NU-PAGE bis-Tris gel (Invitrogen). The proteins from the gels were transferred to a polyvinylidene difluoride (PVDF) membrane (Millipore, Bedford, Mass.). Blots were incubated overnight at 4°C with a mixture of six anti-HIV-1 RT monoclonal antibodies (kind gifts from M. Parniak [24]) and then for 2 h with anti-mouse immunoglobulin G–horseradish peroxidase (Amersham Pharmacia, Piscataway, N.J.). Blots were probed with ECL-Plus (Amersham Pharmacia) and exposed on film (Eastman Kodak, Rochester, N.Y.).

STF-PERT assay. Single-tube fluorescent product-enhanced RT (STF-PERT) assays were performed on supernatants of CEMx174 cells infected with SIV_{mne}, RT-$SHIV_{mne}$, or SIV-RT-YY as described previously (41). Briefly, lysates of viral supernatants were added to RT reaction mixtures containing MS2 RNA template, MS2-specific primer, and deoxynucleoside triphosphates (dNTPs) in 96-well plates. Each RT reaction was separated within the same well by AmpliWax (Applied Biosystems, Foster City, Calif.) from a real-time PCR mixture containing two MS2-specific primers, a fluorescent probe, dNTPs, and AmpliTaq (Applied Biosystems). All samples were run in triplicate in one or two dilutions. A standard curve was created using HIV-1 RT enzyme (Worthington, Lakewood, N.J.) diluted between 10^{-2} and 10^{-10} U/μl in the same buffer used for the samples and assayed in triplicate. The Opticon real-time PCR machine was used to perform the reactions and quantify the amounts of RT per sample. The reaction conditions were 37°C for 89 min (RT reaction); 95°C for 10 min (melting the wax to combine reactions); and 50 cycles of 95°C for 15 s and 56°C for 30 s (PCR).

RT inhibition assays with NRTIs and NNRTIs. JC53 BL13+ cells were seeded at 4×10^4 cells/well in 12-well plates. Cells were challenged in duplicate with HIV-1_{NFNSX} at an MOI of 0.025, and SIV_{mne}, RT-$SHIV_{mne}$, and SIV-RT-YY at an MOI of 0.02 in the presence of 10 μg of DEAE-dextran/ml with or without fivefold dilutions of RT inhibitors. Cells were incubated for 2 h at 37°C and washed with sterile phosphate-buffered saline, received new medium with or without drug added, and were assayed 48 h later. Cellular lysates were prepared according to the manufacturer's instructions and assayed in triplicate with the luciferase assay system (Promega, Madison, Wis.) by using a 1450 Microbeta luminescence counter (EG&G Wallac, Turku, Finland). Results are expressed as luciferase counts per second and are shown as the percent cells infected for each virus with each dilution of drug compared to infection without drug. Fifty percent inhibitory concentration (IC_{50}) values of drugs with each virus were calculated using nonlinear regression with the Prism software (GraphPad, San Diego, Calif.).

sMAGI cells, an SIV indicator cell line (10), were transduced with a murine leukemia virus vector encoding the CCR5 gene and sorted for high cell surface expression of CCR5. The resultant sMAGI-Hi5 cells were plated at 2×10^4 cells/well in a 24-well plate. Cells were challenged with and without drugs as described for JC53 BL13+ cells and stained with X-Gal as described above. Blue cells were counted using an inverted microscope. IC_{50} values of EFV with each virus were calculated as described above.

Selection for NNRTI resistance. CEMx174 cells were infected with RT-$SHIV_{mne}$ at an MOI of 0.02 in 1 ml of medium in 15-ml conical vials at 37°C for 2 h. Cells were transferred to flasks in a total of 5 ml of medium in the presence or absence of EFV, NVP, or UC781. Cells were split every 2 to 3 days and monitored for p27 production. Drug concentrations were increased twofold in new medium every 10 to 14 days until virus production in the presence of drug was similar to that of virus grown without drug.

RNA was extracted from viral supernatants, and RT-PCR was performed using SuperScript one-step RT-PCR (Invitrogen) with the primers 5′-GCAAA AGGATTAAAGGGACAAT-3′ and 5′-GGGTAATCCAAATTTGAATACCA ATTCT-3′ under the following conditions: one cycle of 58°C for 30 min and 94°C for 2 min; 35 cycles of 94°C for 30 s, 60°C for 30 s, and 70°C for 2 min; and one cycle of 72°C for 10 min. PCR products were TA cloned, and multiple colonies were picked and sequenced at the NCI Laboratory of Molecular Technology.

Allele-specific real-time PCR. Viral RNA was isolated from 0.250-ml aliquots of supernatants of the RT-$SHIV_{mne}$-infected cell cultures after each round of selection in the presence or absence of EFV or NVP and converted to cDNA with specific primers. The target sequence region (corresponding to HIV-1_{LAI} *pol* nucleotides 2195 to 2818) was amplified in an Opticon real-time PCR machine, and the total amplified DNA was quantified using SYBR green fluorescence with an appropriate standard curve. The products were diluted to approximately 10^7 total copies per reaction mixture, and a second round of PCR was performed with nondiscriminating primers as well as with primers that amplified specific mutant sequences, using SYBR green fluorescence to detect the amplified product. To minimize the contribution of nonspecific amplification to the fluorescent signal, fluorescence was measured at a temperature just below the T_m of the correct product but above the T_m of small, nonspecific products. To confirm the specificity of amplification, the PCR products were subjected to a melting curve analysis. Samples that did not yield the correct T_m for the amplified product were removed from the analysis. All analyses were done in triplicate, and results are reported as the percent mutant, which was determined by dividing the mutant population detected by the total population detected. Analyses with a coefficient of variation greater than 100% were repeated. Detailed information about this assay will be provided upon request.

RESULTS

Construction and in vitro kinetics of RT-$SHIV_{mne}$ and SIV-RT-YY. We used two approaches to develop SIV_{mne} isolates that were sensitive to NNRTIs. First, SIV_{mne} was modified by replacement of the RT coding region with that of HIV-1_{HXB2}, to yield a virus designated RT-$SHIV_{mne}$. This RT coding region has previously been introduced into the SIV_{mac239} isolate to generate the chimeric virus designated RT-$SHIV_{mac239}$ (46). In the second approach, we made more subtle changes in the RT coding region of SIV_{mne}. Tyrosine residues at amino acid positions 181 and 188 play a significant role in NNRTI sensitivity in HIV-1 RT (40); in SIV_{mne} RT the corresponding amino acids are valine and lysine, respectively. Both residues were changed to tyrosines, and the resulting virus was designated SIV-RT-YY (Fig. 1). Equal amounts of the wild-type

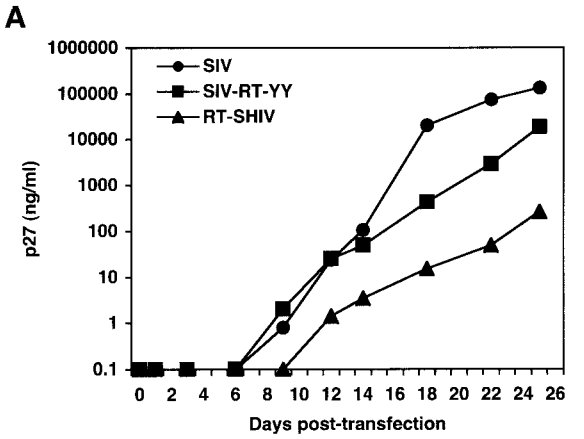

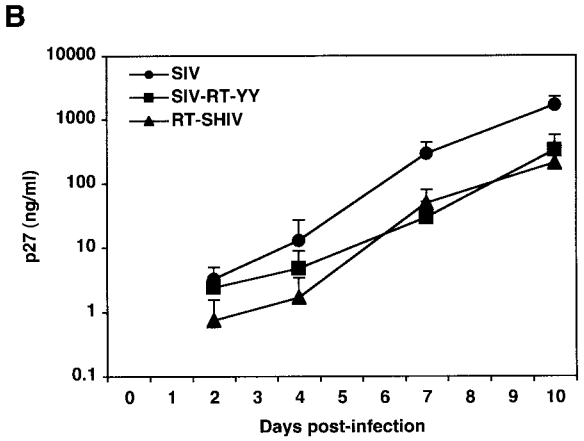

C

Virus	IU/ng CA
SIV	2511
SIV-RT-YY	272
RT-SHIV	178

FIG. 2. In vitro replication kinetics of SIV isolates. (A and B) CEMx174 cell cultures were electroporated with 10 mg of SIV_{mne}, RT-$SHIV_{mne}$, and SIV-RT-YY DNA (A) or infected with an MOI of 0.02 with SIV_{mne}, RT-$SHIV_{mne}$, and SIV-RT-YY (B). SIV_{mne} p27 was used to monitor viral replication. Each time point represents the average of duplicates. Time points for the infections shown in panel B are the average of two independent experiments. (C) The specific infectivity (infectious units per nanogram of p27) of each virus was calculated by dividing the number of infectious units (per milliliter) as determined on JC53 BL+ cells by the amount of p27 (in nanograms per milliliter) at day 7.

SIV_{mne}, RT-$SHIV_{mne}$, and SIV-RT-YY plasmids were introduced into CEMx174 cells by electroporation, and the cells were monitored for the production of virus by p27 ELISA (Fig. 2A). RT-$SHIV_{mne}$ and SIV-RT-YY were produced in cell culture at reduced levels relative to SIV_{mne}.

Portions of the genomes of both mutant viruses were sequenced after 7 weeks of in vitro passaging in CEMx174 cells. The PPT, NC, and IN regions of RT-$SHIV_{mne}$ and SIV-RT-YY were identical to those of wild-type SIV. The RT region, including the junctions between RT, IN, and PR, of RT-$SHIV_{mne}$ was identical to that of HIV-1_{HXB2}. The RT coding region, including junctions, of SIV-RT-YY was identical to that of SIV_{mne} with the exception of the tyrosine substitutions introduced at residues 181 and 188, which were retained (data not shown).

To compare replication efficiencies between the different isolates, RT-$SHIV_{mne}$ and SIV-RT-YY virus supernatants were harvested 5 weeks postelectroporation, titers were determined by limiting dilution on JC53 BL13+ cells, and wild-type SIV_{mne} and the viral variants were used to infect parallel cultures of CEMx174 cells at equal MOIs. RT-$SHIV_{mne}$ and SIV-RT-YY both replicated with similar efficiency based on p27 measurements, and the levels were approximately 10-fold lower than that of wild-type SIV_{mne} (Fig. 2B). For example, using indicator cells, the specific infectivity of each virus at time points during log-phase growth (day 7) was 9- and 14-fold lower for SIV-RT-YY and RT-$SHIV_{mne}$, respectively, compared to that with wild-type virus (Fig. 2C).

HIV-1 RT incorporation and processing in RT-$SHIV_{mne}$ particles. To see if differences in RT incorporation or processing could explain the differences in replication efficiency, we measured the levels of RT and the p66 and p51 cleavage products in RT-$SHIV_{mne}$ and HIV-1 particles. Samples were normalized to viral genomic RNA content. HIV-1 and RT-$SHIV_{mne}$ were concentrated from cell culture supernatants, and the number of RNA genomes was quantified by real-time PCR of a conserved *pol* amplicon present in both genomes. There were 1.5×10^{10} RNA copies/ml in the HIV-1 sample; the RT-$SHIV_{mne}$ sample contained 4.0×10^{10} RNA copies/ml. Solubilized HIV-1 and RT-$SHIV_{mne}$ virus samples were fractionated by sodium dodecyl sulfate-polyacrylamide gel electrophoresis, transferred to a PVDF membrane, and probed with HIV-1 RT-specific monoclonal antibodies (Fig. 3). When the two viruses were diluted to give equivalent amounts of RT, there was threefold less HIV-1 than RT-$SHIV_{mne}$. This suggests that RT-$SHIV_{mne}$ has threefold less RT per RNA ge-

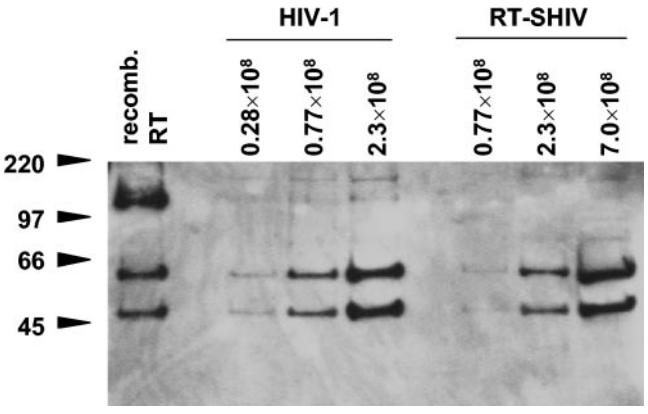

FIG. 3. Immunoblot of HIV-1 RT from HIV-1 and RT-$SHIV_{mne}$ virions. HIV-1_{LAI} and RT-$SHIV_{mne}$ virions were loaded at 0.28×10^8, 0.77×10^8, and 2.3×10^8 RNA copies/ml per lane for HIV-1 and at 0.77×10^8, 2.3×10^8, and 7.0×10^8 RNA copies/ml per lane for RT-$SHIV_{mne}$, as determined by real-time PCR amplification of RT. Recombinant RT was used as a positive control. The larger band is sulfhydryl-cross-linked (oxidized) RT. The gel was transferred to a PVDF membrane and probed with anti-RT monoclonal antibodies, followed by an anti-mouse immunoglobulin G–horseradish peroxidase antibody. Protein size markers are denoted on the left in kilodaltons.

TABLE 1. RT activity per p27 of the SIV isolates

Virus	% RT[a]		Avg % RT[b]	p27 (μg/ml)	RT/p27[c]	Fold difference[d]
	Expt 1	Expt 2				
SIV_{mne}	100	100	100	0.2	440	
RT-$SHIV_{mne}$	49	28	39 ± 15	0.1	290	1.5
SIV-RT-YY	11	10	10 ± 1	0.04	280	1.6

[a] Amount of RT in mutant viruses compared to wild-type SIV_{mne} in two independent experiments at day 10 postinfection.
[b] Average and standard deviation of RT activity from the two experiments.
[c] RT activity per p27 was calculated by dividing the amount of RT by the amount of p27.
[d] Fold difference of RT/p27 ratio between SIV_{mne} and the mutant viruses.

nome, and presumably per virion. For both HIV-1 and RT-$SHIV_{mne}$, similar ratios of p66 and p51 subunits of RT were present in the virus preparations, suggesting that HIV-1 RT is cleaved efficiently by SIV protease in RT-$SHIV_{mne}$.

RT activity of SIV_{mne} and mutant viruses. Because it would be difficult to compare absolute levels of SIV and HIV-1 RT molecules present in SIV_{mne} and RT-$SHIV_{mne}$ particles, we employed the sensitive STF-PERT assay (41) to quantify the RT activity in supernatants of infected CEMx174 cells. The STF-PERT assay is linear over 8 orders of magnitude and displays minimal interassay variance between redundant samples within a single run (41). Because the SIV-RT-YY virus replicated less well than the wild-type virus, we also assayed the relative RT activity of this mutant. The RT activities of RT-$SHIV_{mne}$ and SIV-RT-YY supernatants were 40 and 10% of that of wild-type SIV_{mne}, respectively, reflecting diminished replication by the mutant viruses (Table 1). The RT activity per p27 of SIV_{mne} during log-phase growth was, on average, 1.5-fold higher than that of the mutant viruses.

Sensitivity of mutant viruses to NRTIs and NNRTIs. To evaluate the sensitivity to RT inhibitors of the two mutant viruses relative to that of HIV-1 and wild-type SIV_{mne}, we measured replication in the presence or absence of dilutions of various NRTIs. JC53 BL13+ indicator cells were challenged with HIV-1, SIV_{mne}, RT-$SHIV_{mne}$, and SIV-RT-YY in the presence and absence of various concentrations of several NRTIs: AZT, d4T, ddI, 3TC, and tenofovir. IC_{50} values were determined for each virus with each drug and were similar for all four viruses for each drug (Table 2). These values were not significantly different from those determined by others using different assays with HIV-1 isolates (3, 4, 8, 9, 32).

Next, the indicator cells were challenged with HIV-1, SIV_{mne}, RT-$SHIV_{mne}$, and SIV-RT-YY in the presence and absence of different concentrations of the NNRTIs EFV, NVP, and UC781 (Fig. 4). Table 3 shows the range of IC_{50} values determined for each virus with each of the NNRTIs. As expected, HIV-1 was inhibited by all three NNRTIs, while SIV_{mne} was either not inhibited or inhibited to a much lesser extent than HIV-1. If anything, RT-$SHIV_{mne}$ replication was more sensitive to inhibition by EFV, NVP, and UC781 than HIV-1. In contrast, SIV-RT-YY was only partially inhibited by EFV (the IC_{50} was 70-fold higher than that for HIV-1). The SIV-RT-YY virus showed no appreciable inhibition by the other NNRTIs; the IC_{50} values for NVP and UC781 were similar to those for SIV_{mne}. Because these assays were performed with a human cell line, we also tested the antiviral potency of EFV in macaque cells. Similar results were obtained with HIV-1, SIV_{mne}, and RT-$SHIV_{mne}$ in the presence of EFV by using sMAGI-Hi5 cells, a macaque indicator cell line (Fig. 5). Thus, RT-$SHIV_{mne}$ was at least as sensitive, if not more sensitive, to NNRTIs as HIV-1.

Development of NNRTI resistance mutations in RT-$SHIV_{mne}$. To determine the spectrum of resistance mutations that arise in RT-$SHIV_{mne}$ in response to NNRTI treatment, RT-$SHIV_{mne}$ was grown in the presence of increasing concentrations of EFV, NVP, and UC781, and NNRTI-resistant viruses were selected. The accumulation of SIV p27 CA was monitored in cell culture supernatants (data not shown), and virus was harvested from cultures maintained in high concentrations of NNRTIs. The RT gene was sequenced from these viruses, and multiple mutations were found in viruses selected for each drug (Table 4). All of the RT mutations found in the RT-$SHIV_{mne}$ have been seen in isolates from individuals infected with drug-resistant HIV-1 (Stanford HIV Drug Resistance Database [http://hivdb.stanford.edu/]), including the K103N and Y181C mutations, which are commonly selected in patients.

In addition to bulk sequencing of RT-$SHIV_{mne}$ isolated from culture supernatants of cells grown in the presence or absence of NNRTIs, the kinetics and appearance of the K103N and Y181C mutations were determined by allele-specific real-time RT-PCR. Viral RNA was isolated from RT-$SHIV_{mne}$-infected cells after each increase in concentration of EFV or NVP and from parallel cultures without selection. 103N-specific primers were used for EFV-selected virus (Fig. 6A), while 181C-specific primers were used for NVP-selected virus (Fig. 6B). The proportion of both mutations increased over time as the concentrations of both drugs were added to the RT-$SHIV_{mne}$-infected cells. RT-$SHIV_{mne}$ grown in cells without drug did not contain significant amounts of K103N or Y181C.

TABLE 2. Summary of virus inhibition with NRTIs

Drug	Reference IC_{50} range (nM)[a]	IC_{50} (nM) in JC53 BL13+ cells[b]			
		HIV-1	SIV_{mne}	RT-$SHIV_{mne}$	SIV-RT-YY
AZT	10–40	37 ± 22	48 ± 53	56 ± 24	51 ± 8
ddI	2,500–15,800	10,600 ± 7,600	8,200 ± 4,900	15,800 ± 18,400	14,400 ± 14,600
d4T	340–2,100	2,300 ± 2,500	830 ± 500	1,200 ± 93	2,500 ± 3,500
3TC	780–1,500	1,200 ± 87	1,700 ± 740	1,110 ± 440	2,500 ± 1,900
Tenofovir	880–1,900	2,100 ± 170	790 ± 250	1,200 ± 380	770 ± 190

[a] Reference IC_{50} values were determined for HIV-1 in previous studies (32).
[b] Values indicate the average and standard deviation of values from two to three independent experiments.

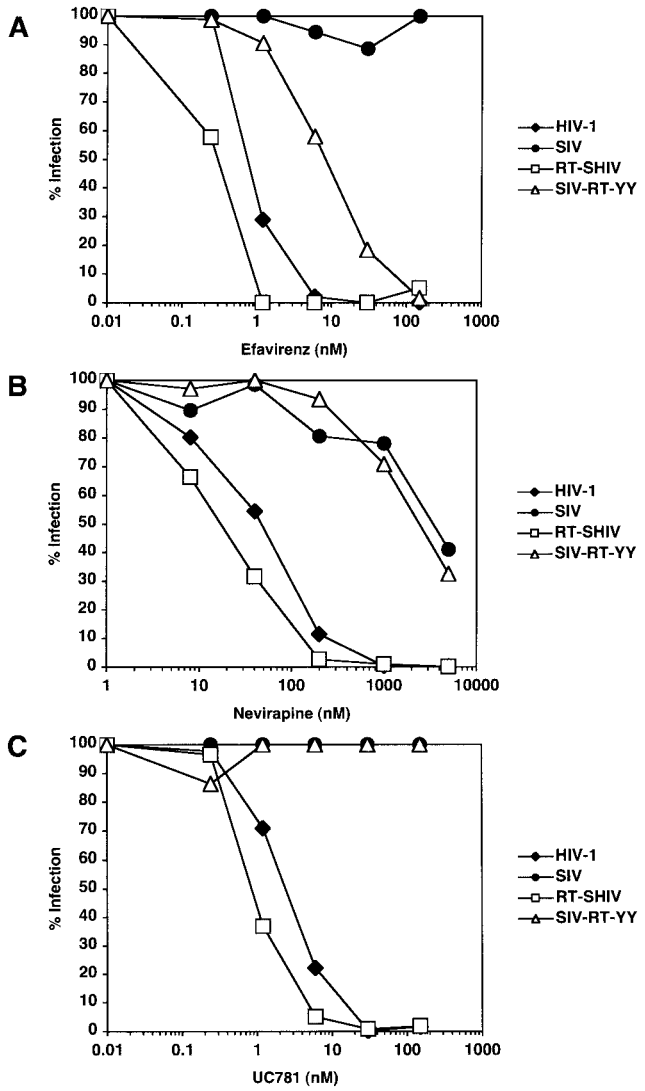

FIG. 4. In vitro RT inhibition with NNRTIs. Representative data are shown in which JC53 BL13+ cells were infected with HIV-1_{NFNSX}, SIV_{mne}, RT-$SHIV_{mne}$, or SIV-RT-YY in the presence or absence of multiple concentrations of EFV (A), NVP (B), or UC781 (C). Infections were performed in duplicate, and luciferase measurements were performed in triplicate. Results are expressed as the percent cells infected for each virus with each dilution of drug compared to infection without drug.

DISCUSSION

Animal models that can be used to study the development of HIV-1 antiviral resistance have the potential to provide important insights relating to the fitness of drug-resistant isolates and the efficacy of inhibitors in different tissues and cell types. To help address this need, we have developed a SIV chimeric virus for infection of pigtail macaques that should be suitable for in vivo analyses of NNRTI therapies. A SIV_{mne} that replicated using HIV-1 RT was as susceptible as HIV-1 to NNRTIs. In contrast, a mutant SIV_{mne} with amino acids 181 and 188 replaced with tyrosine residues displayed partial sensitivity to EFV only.

Both the replacement of specific amino acids at positions 181 and 188 and the replacement of the entire RT coding region of SIV_{mne} with those of HIV-1 led to approximately a 10-fold reduction in the replication of the viruses. Consistent with these findings, others have reported diminished replication or RT activity in SIV_{mac239} or $HIV\text{-}2_{ROD}$ when amino acids 176 to 190 or 188 alone were changed to the corresponding residues found in the HIV-1 RT (17, 18, 43). Recent crystal structure analysis of the HIV-2 RT in the presence and absence of NNRTIs suggests that differences in amino acid residues near the active site, including those at positions 181 and 188, could result in significant changes in side chain steric hindrance, electrostatic properties, and positioning of the residues (34). The substitution of tyrosines at positions 181 and 188 could distort the active site and/or the position of the nucleic acid relative to the active site and affect the activity of the enzyme.

The decrease in replication of RT-$SHIV_{mne}$ is reminiscent of RT-$SHIV_{mac239}$ with a compensatory mutation at the viral tRNA-Lys3 PBS (1, 46). In the absence of this compensatory mutation, the replication of RT-$SHIV_{mac239}$ appears to be severely impaired. Prior reports indicated that RT-$SHIV_{mac239}$ was undetectable in CEMx174 cell culture supernatants for up to 65 days in the absence of such a mutation (44). Because RT-$SHIV_{mne}$ possesses a canonical tRNA-Lys3 PBS, our results suggest that other adaptive changes may be required for optimal replication of these chimeric viruses.

The reduced replication of RT-$SHIV_{mne}$ and SIV-RT-YY

TABLE 3. Summary of virus inhibition with NNRTIs

Drug	Reference range (nM)[a]	IC_{50} (nM) in JC53 BL13+ cells[b]			
		HIV-1	SIV_{mne}	RT-$SHIV_{mne}$	SIV-RT-YY
EFV	0.6–3.6	0.5 ± 0.3	>150	0.25 ± 0.07	7 ± 3
NVP	23–142	48 ± 1	2,300 ± 2,500	22 ± 2	2,600 ± 890
UC781	5–10.4	2 ± 0.5	>150	0.9 ± 0.8	>150

[a] Reference IC_{50} values determined for HIV-1 in previous studies (3, 4, 8, 9, 32).
[b] Values indicate the average and standard deviation of values from two to three independent experiments similar to those shown in Fig. 4.

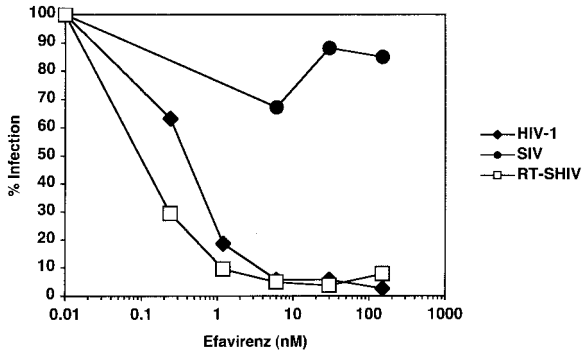

FIG. 5. In vitro RT inhibition in macaque cells with EFV. sMAGI-Hi5 cells were infected with HIV-1_{NFNSX}, SIV_{mne}, and RT-$SHIV_{mne}$ in the presence or absence of various concentrations of EFV. Infections were performed in duplicate, and blue cells (infectious centers) were counted. Results are expressed as the percent cells infected for each virus with each dilution of drug compared to infection without drug. IC_{50} values in this assay were as follows: 0.4 nM for HIV-1, >150 nM for SIV_{mne}, <0.2 nM for RT-$SHIV_{mne}$, and 8.5 nM for SIV-RT-YY.

TABLE 4. RT mutations found in NNRTI-selected RT-SHIV$_{mne}$

Drug (no. of clones)	Mutations in RT-SHIV$_{mne}$[a]
EFV (12)	**P1L, K103N, E194K**
NVP (8)	E36G, **Y181C**, D237N, R358K
UC781 (10)	V179D, E194K

[a] Mutations seen in three or more clones are listed, with those seen in the majority of the clones indicated in bold.

compared to wild-type SIV$_{mne}$ is due to diminished RT activity. By quantifying the RT activity in virus from CEMx174 cells, we found that the amount of RT activity per particle of RT-SHIV$_{mne}$ was approximately 40% less than that of SIV$_{mne}$ in a quantitative STF-PERT assay. Previous studies have indicated that the polymerase activity of HIV-2 RT, a protein highly homologous to SIV RT, is not significantly different than that of HIV-1 RT in the presence of high levels of dNTPs (14). This suggests that an RT-SHIV$_{mne}$ virion, which encodes wild-type HIV-1 RT, contains less mature RT than a wild-type SIV$_{mne}$ virion. SIV-RT-YY also has a 1.5-fold-lower RT/p27 ratio than SIV$_{mne}$, which could reflect either a processing defect or lower enzymatic activity of the mutant RT.

HIV-1 RT cleavage into p66 and p51 subunits in RT-SHIV$_{mne}$ is dependent on SIV protease. The amount of RT subunits in RT-SHIV$_{mac239}$ had not been measured quantitatively; thus, we examined whether inefficiencies in the folding or processing of RT could account for differences in viral replication efficiency. The reduced replication of RT-SHIV$_{mne}$ did not appear to be due to inefficient cleavage of RT into p66 and p51 subunits by SIV protease, since immunoblot analysis of HIV-1 and RT-SHIV$_{mne}$ particles showed similar ratios of p66 to p51 for the two viruses. However, in the course of this analysis, we noted that the total amount of RT in RT-SHIV$_{mne}$ virions was lower than in HIV-1 virions, which correlated with the lower amount of RT activity of RT-SHIV$_{mne}$ virions compared to wild-type SIV$_{mne}$ virions.

The reduction in the amount of RT in the RT-SHIV$_{mne}$ particles corresponds to the lower replication of the virus. Previous work in which cells were cotransfected with different ratios of HIV-1 vectors encoding wild-type RT or an RT lacking polymerase activity showed that a decrease in virion particle RT activity caused a significant reduction in replication (19). When wild-type RT was reduced to 50 or 25% of levels in wild-type particles, the relative infectivity of the virus was 42 and 3%, respectively. RT-SHIV$_{mne}$ virions appear to incorporate approximately 30% of the RT found in HIV-1 virions, and RT-SHIV$_{mne}$ replicates to a titer approximately 7% that of wild-type SIV$_{mne}$, consistent with the HIV-1 studies.

There are several possible explanations for the reduced amount of RT protein per virion in RT-SHIV$_{mne}$. The chimeric p160$^{gag\text{-}pol}$ polyprotein may be expressed inefficiently by reduced frameshifting. The mutant polyprotein could also be folded inefficiently in cells, promoting its degradation. It is also possible that HIV-1 RT could be degraded in RT-SHIV$_{mne}$ particles by the SIV protease, although RT degradation products were not detected in our immunoblot analyses of RT-SHIV$_{mne}$. Alternatively, it is conceivable that the RT-SHIV$_{mne}$ p160$^{gag\text{-}pol}$ precursor either does not traffic efficiently to sites of SIV Gag assembly or is less efficiently incorporated into virion particles. Previous studies have reported that there are mutations in HIV-1 RT that interfere with the incorporation and/or processing of p160$^{gag\text{-}pol}$ and that these mutations lead to a reduction in RT activity (16).

Normalizing virus in supernatants based on viral RNA content using the same sequence in the *pol* gene of HIV-1 and RT-SHIV$_{mne}$ has advantages over other approaches for quantifying virions. For instance, ELISA analysis of the CA content of HIV-1 and RT-SHIV$_{mne}$ required the use of different immunological reagents with different sensitivities, and electron microscopy determination of particle counts was difficult because of extensive microvesicle contamination (data not shown). Implicit in the use of real-time RT-PCR detection to quantify the viruses is the assumption that, on average, equal amounts of viral genome RNA copies are present in HIV-1 and RT-SHIV$_{mne}$ particles. Nonetheless, these data clearly show that the ratio of RT to viral genome RNA is different between HIV-1 and RT-SHIV$_{mne}$.

In spite of their reduced replication, RT-SHIV$_{mne}$ and SIV-RT-YY showed equivalent sensitivities to HIV-1 and SIV$_{mne}$

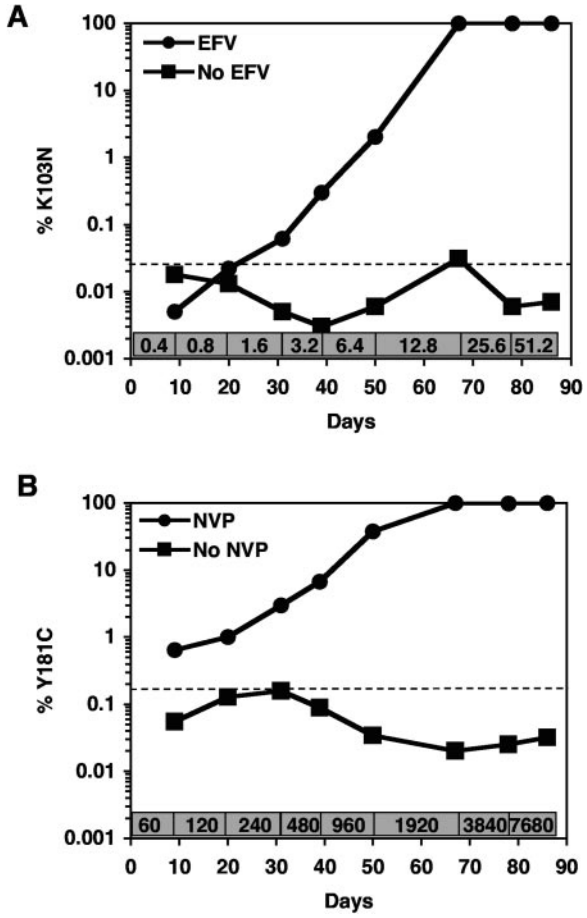

FIG. 6. Proportion of specific NNRTI resistance mutations in RT-SHIV$_{mne}$ selected in the presence or absence of NNRTIs. Virus selected in CEMx174 cells grown in the presence or absence of increasing concentrations of EFV (A) or NVP (B) was assayed by allele-specific real-time RT-PCR for quantitation of the mutations K103N or Y181C, respectively. The concentration (nanomolar) of each drug during the selection of the cultures is denoted at the bottom of each graph. The dashed lines indicate the background of the assays: 0.0265% ± 0.007% (K103N) and 0.169% ± 0.017% (Y181C).

with several NRTIs. As predicted, the presence of HIV-1 RT in SIV_{mne} makes RT-$SHIV_{mne}$ susceptible to EFV, NVP, and UC781. RT-$SHIV_{mne}$ appeared to be slightly more sensitive to EFV, NVP, and UC781 than HIV-1. Hypersensitivity of HIV-1 to NNRTIs has been detected in 17% of patient plasma samples, is more common for EFV than NVP, and is associated with certain NRTI resistance mutations (48). We did not detect any mutations in RT-$SHIV_{mne}$ that would explain its increased susceptibility to NNRTIs. NRTIs inhibit reverse transcription by interfering with synthesis of the viral genome, whereas NNRTIs inhibit reverse transcription by binding to the RT enzyme itself. However, the level of RT in a virus particle will affect NNRTI sensitivity. If excess RT is present it can bind the drug, but replication can still occur. In contrast, the target for NRTI inhibition is the viral genome, not RT, and the level of RT will not affect NRTI susceptibility. Thus, the decrease in the amounts of RT in the RT-$SHIV_{mne}$ virions could make these virions more sensitive to inhibition by NNRTIs but not NRTIs.

Mutation of residues 181 and 188 to tyrosines in SIV_{mne} increased the sensitivity of the virus to EFV but did not make it as sensitive as HIV-1. This result is in accord with structural data that show that other residues are important in binding these drugs, especially NVP and UC781. Replacement of residues 176 to 190 of RT increased the sensitivity of $HIV\text{-}2_{ROD}$ and SIV_{mac239} to NVP to levels three- to fourfold higher than the IC_{50} value for HIV-1 (18, 42, 43). Loss of tyrosines at positions 181 and/or 188 of HIV-1 RT reduced the inhibition by first-generation NNRTIs, including NVP (11, 15). However, the second-generation NNRTI EFV does interact with the tyrosine at 188 in HIV-1 RT, but it has minimal contact with the tyrosine at 181 (15), which may explain the better efficacy of EFV against SIV-RT-YY. Our data reinforce the notion that the specific tertiary structure of HIV-1 RT targeted by NNRTIs is difficult to recreate even in related molecules.

Selection of NNRTI-resistant RT-$SHIV_{mne}$ in vitro leads to RT mutations that are seen in patients infected with drug-resistant HIV-1. Mutations commonly associated with NNRTI resistance were seen in RT-$SHIV_{mne}$ after selection with EFV, NVP, and UC781: K103N, V179D, Y181C, and E194K (2). It is possible that the unusual P1L mutation that arises in RT-$SHIV_{mne}$ selected with EFV increases the amount of RT in the virions, by affecting the folding and/or processing of the $p160^{gag\text{-}pol}$ precursor, which would contribute to the resistant phenotype. Using our assay for detection of specific mutations in viral RNA, we can see the proportion of K103N and Y181C resistance mutations increase as RT-$SHIV_{mne}$ replicates in the presence of escalating doses of EFV and NVP, respectively. These mutations do not appear in virus that is not selected with drugs. This assay will be useful in examining the relative fitness of K103N or Y181C resistance mutations within an animal model in the presence and absence of antiviral selection.

Currently, few studies have been performed in which macaques have been infected with RT-$SHIV_{mac239}$ and treated with NNRTIs (28, 46, 49), and only one study evaluated the development of drug resistance mutations in RT after treatment with NVP (49). More recently, an RT-SHIV based on the SIV_{mac239} molecular clone was developed that also included the *vpr*, *vpu*, *tat*, *rev*, *env*, and *nef* genes from $HIV\text{-}1_{NL4\text{-}3}$ (1). However, replication of this chimeric virus was not detectable in two rhesus macaques 6 and 12 weeks postinoculation, and the susceptibility of this chimera to RT inhibitors was not directly compared to HIV-1 in cell culture. Additional models whose replication and drug-resistant properties have been extensively characterized in vitro may yield more reliable alternatives for in vivo studies. An RT-$SHIV_{mne}$/pigtail macaque model that recapitulates the immunopathogenesis, persistence, and systemic distribution of HIV-1 would provide an important tool in the design of clinical treatment regimens to help minimize the development of antiviral drug resistance.

ACKNOWLEDGMENTS

We thank Jörg Baumann, Arifa Khan, and Jane Mirro for technical advice and assistance; Paul Boyer, Gisela Heidecker, John Kappes, and Klaus Überla for reagents; and Stuart Le Grice, Jason Kimata, Jeff Lifson, Frank Maldarelli, John Mellors, and Alan Rein for helpful discussions.

Funding for this research was provided by the National Cancer Institute's intramural Center for Cancer Research, which supports the HIV Drug Resistance Program. Z.A. is supported by an American Foundation for AIDS Research (amfAR) postdoctoral fellowship.

The content of this publication does not necessarily reflect the views or policies of the Department of Health and Human Services, nor does mention of trade names, commercial products, or organizations imply endorsement by the U.S. Government.

REFERENCES

1. **Akiyama, H., E. Ido, W. Akahata, T. Kuwata, T. Miura, and M. Hayami.** 2003. Construction and in vivo infection of a new simian/human immunodeficiency virus chimera containing the reverse transcriptase gene and the 3′ half of the genomic region of human immunodeficiency virus type 1. J. Gen. Virol. **84:**1663–1669.
2. **Balzarini, J.** 1999. Suppression of resistance to drugs targeted to human immunodeficiency virus reverse transcriptase by combination therapy. Biochem. Pharmacol. **58:**1–27.
3. **Balzarini, J., W. G. Brouwer, D. C. Dao, E. M. Osika, and E. De Clercq.** 1996. Identification of novel thiocarboxanilide derivatives that suppress a variety of drug-resistant mutant human immunodeficiency virus type 1 strains at a potency similar to that for wild-type virus. Antimicrob. Agents Chemother. **40:**1454–1466.
4. **Balzarini, J., L. Naesens, E. Verbeken, M. Laga, L. Van Damme, M. Parniak, L. Van Mellaert, J. Anne, and E. De Clercq.** 1998. Preclinical studies on thiocarboxanilide UC-781 as a virucidal agent. AIDS **12:**1129–1138.
5. **Balzarini, J., M. Weeger, M. J. Camarasa, E. De Clercq, and K. Uberla.** 1995. Sensitivity/resistance profile of a simian immunodeficiency virus containing the reverse transcriptase gene of human immunodeficiency virus type 1 (HIV-1) toward the HIV-1-specific non-nucleoside reverse transcriptase inhibitors. Biochem. Biophys. Res. Commun. **211:**850–856.
6. **Benveniste, R. E., W. R. Morton, E. A. Clark, C. C. Tsai, H. D. Ochs, J. M. Ward, L. Kuller, W. B. Knott, R. W. Hill, M. J. Gale, et al.** 1988. Inoculation of baboons and macaques with simian immunodeficiency virus/Mne, a primate lentivirus closely related to human immunodeficiency virus type 2. J. Virol. **62:**2091–2101.
7. **Benveniste, R. E., S. T. Roodman, R. W. Hill, W. B. Knott, J. L. Ribas, M. G. Lewis, and G. A. Eddy.** 1994. Infectivity of titered doses of simian immunodeficiency virus clone E11S inoculated intravenously into rhesus macaques (Macaca mulatta). J. Med. Primatol. **23:**83–88.
8. **Borkow, G., D. Arion, M. A. Wainberg, and M. A. Parniak.** 1999. The thiocarboxanilide nonnucleoside inhibitor UC781 restores antiviral activity of 3′-azido-3′-deoxythymidine (AZT) against AZT-resistant human immunodeficiency virus type 1. Antimicrob. Agents Chemother. **43:**259–263.
9. **Borkow, G., J. Barnard, T. M. Nguyen, A. Belmonte, M. A. Wainberg, and M. A. Parniak.** 1997. Chemical barriers to human immunodeficiency virus type 1 (HIV-1) infection: retrovirucidal activity of UC781, a thiocarboxanilide nonnucleoside inhibitor of HIV-1 reverse transcriptase. J. Virol. **71:**3023–3030.
10. **Chackerian, B., N. L. Haigwood, and J. Overbaugh.** 1995. Characterization of a CD4-expressing macaque cell line that can detect virus after a single replication cycle and can be infected by diverse simian immunodeficiency virus isolates. Virology **213:**386–394.
11. **Das, K., J. Ding, Y. Hsiou, A. D. Clark, Jr., H. Moereels, L. Koymans, K. Andries, R. Pauwels, P. A. Janssen, P. L. Boyer, P. Clark, R. H. Smith, Jr., M. B. Kroeger Smith, C. J. Michejda, S. H. Hughes, and E. Arnold.** 1996. Crystal structures of 8-Cl and 9-Cl TIBO complexed with wild-type HIV-1 RT and 8-Cl TIBO complexed with the Tyr181Cys HIV-1 RT drug-resistant mutant. J. Mol. Biol. **264:**1085–1100.

12. **Derdeyn, C. A., J. M. Decker, J. N. Sfakianos, X. Wu, W. A. O'Brien, L. Ratner, J. C. Kappes, G. M. Shaw, and E. Hunter.** 2000. Sensitivity of human immunodeficiency virus type 1 to the fusion inhibitor T-20 is modulated by coreceptor specificity defined by the V3 loop of gp120. J. Virol. **74:**8358–8367.
13. **Heidecker, G., H. Munoz, P. Lloyd, D. Hodge, F. W. Ruscetti, W. R. Morton, S. Hu, and R. E. Benveniste.** 1998. Macaques infected with cloned simian immunodeficiency virus show recurring nef gene alterations. Virology **249:**260–274.
14. **Hizi, A., R. Tal, M. Shaharabany, and S. Loya.** 1991. Catalytic properties of the reverse transcriptases of human immunodeficiency viruses type 1 and type 2. J. Biol. Chem. **266:**6230–6239.
15. **Hsiou, Y., K. Das, J. Ding, A. D. Clark, Jr., J. P. Kleim, M. Rosner, I. Winkler, G. Riess, S. H. Hughes, and E. Arnold.** 1998. Structures of Tyr188Leu mutant and wild-type HIV-1 reverse transcriptase complexed with the non-nucleoside inhibitor HBY 097: inhibitor flexibility is a useful design feature for reducing drug resistance. J. Mol. Biol. **284:**313–323.
16. **Huang, W., A. Gamarnik, K. Limoli, C. J. Petropoulos, and J. M. Whitcomb.** 2003. Amino acid substitutions at position 190 of human immunodeficiency virus type 1 reverse transcriptase increase susceptibility to delavirdine and impair virus replication. J. Virol. **77:**1512–1523.
17. **Isaka, Y., S. Miki, S. Kawauchi, A. Suyama, H. Sugimoto, A. Adachi, T. Miura, M. Hayami, O. Yoshie, T. Fujiwara, and A. Sato.** 2001. A single amino acid change at Leu-188 in the reverse transcriptase of HIV-2 and SIV renders them sensitive to non-nucleoside reverse transcriptase inhibitors. Arch. Virol. **146:**743–755.
18. **Isaka, Y., A. Sato, S. Kawauchi, A. Suyama, S. Miki, M. Hayami, and T. Fujiwara.** 1998. Construction of the chimeric reverse transcriptase of simian immunodeficiency virus sensitive to nonnucleoside reverse transcriptase inhibitor. Microbiol. Immunol. **42:**195–202.
19. **Julias, J. G., A. L. Ferris, P. L. Boyer, and S. H. Hughes.** 2001. Replication of phenotypically mixed human immunodeficiency virus type 1 virions containing catalytically active and catalytically inactive reverse transcriptase. J. Virol. **75:**6537–6546.
20. **Kimata, J. T., J. J. Gosink, V. N. KewalRamani, L. M. Rudensey, D. R. Littman, and J. Overbaugh.** 1999. Coreceptor specificity of temporal variants of simian immunodeficiency virus Mne. J. Virol. **73:**1655–1660.
21. **Kimata, J. T., L. Kuller, D. B. Anderson, P. Dailey, and J. Overbaugh.** 1999. Emerging cytopathic and antigenic simian immunodeficiency virus variants influence AIDS progression. Nat. Med. **5:**535–541.
22. **Kimpton, J., and M. Emerman.** 1992. Detection of replication-competent and pseudotyped human immunodeficiency virus with a sensitive cell line on the basis of activation of an integrated beta-galactosidase gene. J. Virol. **66:**2232–2239.
23. **Lee, P. P., and M. L. Linial.** 1994. Efficient particle formation can occur if the matrix domain of human immunodeficiency virus type 1 Gag is substituted by a myristylation signal. J. Virol. **68:**6644–6654.
24. **Li, X., E. Amandoron, M. A. Wainberg, and M. A. Parniak.** 1993. Generation and characterization of murine monoclonal antibodies reactive against N-terminal and other regions of HIV-1 reverse transcriptase. J. Med. Virol. **39:**251–259.
25. **Little, S. J., S. Holte, J. P. Routy, E. S. Daar, M. Markowitz, A. C. Collier, R. A. Koup, J. W. Mellors, E. Connick, B. Conway, M. Kilby, L. Wang, J. M. Whitcomb, N. S. Hellmann, and D. D. Richman.** 2002. Antiretroviral-drug resistance among patients recently infected with HIV. N. Engl. J. Med. **347:**385–394.
26. **Mori, K., D. J. Ringler, and R. C. Desrosiers.** 1993. Restricted replication of simian immunodeficiency virus strain 239 in macrophages is determined by env but is not due to restricted entry. J. Virol. **67:**2807–2814.
27. **Mori, K., D. J. Ringler, T. Kodama, and R. C. Desrosiers.** 1992. Complex determinants of macrophage tropism in env of simian immunodeficiency virus. J. Virol. **66:**2067–2075.
28. **Mori, K., Y. Yasutomi, S. Sawada, F. Villinger, K. Sugama, B. Rosenwith, J. L. Heeney, K. Uberla, S. Yamazaki, A. A. Ansari, and H. Rubsamen-Waigmann.** 2000. Suppression of acute viremia by short-term postexposure prophylaxis of simian/human immunodeficiency virus SHIV-RT-infected monkeys with a novel reverse transcriptase inhibitor (GW420867) allows for development of potent antiviral immune responses resulting in efficient containment of infection. J. Virol. **74:**5747–5753.
29. **Morton, W. R., L. Kuller, R. E. Benveniste, E. A. Clark, C. C. Tsai, M. J. Gale, M. E. Thouless, J. Overbaugh, and M. G. Katze.** 1989. Transmission of the simian immunodeficiency virus SIVmne in macaques and baboons. J. Med. Primatol. **18:**237–245.
30. **National Center for Research Resources.** 2002. Rhesus monkey demands in biomedical research: a workshop report. National Center for Research Resources, National Institutes of Health, Bethesda, Md.
31. **O'Brien, W. A., Y. Koyanagi, A. Namazie, J. Q. Zhao, A. Diagne, K. Idler, J. A. Zack, and I. S. Chen.** 1990. HIV-1 tropism for mononuclear phagocytes can be determined by regions of gp120 outside the CD4-binding domain. Nature **348:**69–73.
32. **Palmer, S., R. W. Shafer, and T. C. Merigan.** 1999. Highly drug-resistant HIV-1 clinical isolates are cross-resistant to many antiretroviral compounds in current clinical development. AIDS **13:**661–667.
33. **Palmer, S., A. P. Wiegand, F. Maldarelli, H. Bazmi, J. M. Mican, M. Polis, R. L. Dewar, A. Planta, S. Liu, J. A. Metcalf, J. W. Mellors, and J. M. Coffin.** 2003. New real-time reverse transcriptase-initiated PCR assay with single-copy sensitivity for human immunodeficiency virus type 1 RNA in plasma. J. Clin. Microbiol. **41:**4531–4536.
34. **Ren, J., L. E. Bird, P. P. Chamberlain, G. B. Stewart-Jones, D. I. Stuart, and D. K. Stammers.** 2002. Structure of HIV-2 reverse transcriptase at 2.35-A resolution and the mechanism of resistance to non-nucleoside inhibitors. Proc. Natl. Acad. Sci. USA **99:**14410–14415.
35. **Rittinger, K., G. Divita, and R. S. Goody.** 1995. Human immunodeficiency virus reverse transcriptase substrate-induced conformational changes and the mechanism of inhibition by nonnucleoside inhibitors. Proc. Natl. Acad. Sci. USA **92:**8046–8049.
36. **Rosenberg, Y. J., A. Shafferman, B. D. White, S. F. Papermaster, E. Leon, G. A. Eddy, R. Benveniste, D. S. Burke, and M. G. Lewis.** 1992. Variation in the $CD4^+$ and $CD8^+$ populations in lymph nodes does not reflect that in the blood during SIVMNE/E11S infection of macaques. J. Med. Primatol. **21:**131–137.
37. **Rosenwirth, B., W. M. Bogers, I. G. Nieuwenhuis, P. T. Haaft, H. Niphuis, E. M. Kuhn, N. Bischofberger, V. Erfle, G. Sutter, P. Berglund, P. Liljestrom, K. Uberla, and J. L. Heeney.** 1999. An anti-HIV strategy combining chemotherapy and therapeutic vaccination. J. Med. Primatol. **28:**195–205.
38. **Rudensey, L. M., J. T. Kimata, R. E. Benveniste, and J. Overbaugh.** 1995. Progression to AIDS in macaques is associated with changes in the replication, tropism, and cytopathic properties of the simian immunodeficiency virus variant population. Virology **207:**528–542.
39. **Rudensey, L. M., J. T. Kimata, E. M. Long, B. Chackerian, and J. Overbaugh.** 1998. Changes in the extracellular envelope glycoprotein of variants that evolve during the course of simian immunodeficiency virus SIVMne infection affect neutralizing antibody recognition, syncytium formation, and macrophage tropism but not replication, cytopathicity, or CCR-5 coreceptor recognition. J. Virol. **72:**209–217.
40. **Schinazi, R. F., B. A. Larder, and J. W. Mellors.** 2000. Mutations in retroviral genes associated with drug resistance: 2000–2001 update. Int. Antivir. News **8:**65–91.
41. **Sears, J. F., and A. S. Khan.** 2003. Single-tube fluorescent product-enhanced reverse transcriptase assay with Ampliwax (STF-PERT) for retrovirus quantitation. J. Virol. Methods **108:**139–142.
42. **Shaharabany, M., and A. Hizi.** 1992. The catalytic functions of chimeric reverse transcriptases of human immunodeficiency viruses type 1 and type 2. J. Biol. Chem. **267:**3674–3678.
43. **Shih, C. K., J. M. Rose, G. L. Hansen, J. C. Wu, A. Bacolla, and J. A. Griffin.** 1991. Chimeric human immunodeficiency virus type 1/type 2 reverse transcriptases display reversed sensitivity to nonnucleoside analog inhibitors. Proc. Natl. Acad. Sci. USA **88:**9878–9882.
44. **Soderberg, K., L. Denekamp, S. Nikiforow, K. Sautter, R. C. Desrosiers, and L. Alexander.** 2002. A nucleotide substitution in the tRNA(Lys) primer binding site dramatically increases replication of recombinant simian immunodeficiency virus containing a human immunodeficiency virus type 1 reverse transcriptase. J. Virol. **76:**5803–5806.
45. **Spence, R. A., W. M. Kati, K. S. Anderson, and K. A. Johnson.** 1995. Mechanism of inhibition of HIV-1 reverse transcriptase by nonnucleoside inhibitors. Science **267:**988–993.
46. **Uberla, K., C. Stahl-Hennig, D. Bottiger, K. Matz-Rensing, F. J. Kaup, J. Li, W. A. Haseltine, B. Fleckenstein, G. Hunsmann, B. Oberg, et al.** 1995. Animal model for the therapy of acquired immunodeficiency syndrome with reverse transcriptase inhibitors. Proc. Natl. Acad. Sci. USA **92:**8210–8214.
47. **Volberding, P. A.** 2003. HIV therapy in 2003: consensus and controversy. AIDS **17**(Suppl. 1)**:**S4–S11.
48. **Whitcomb, J. M., W. Huang, K. Limoli, E. Paxinos, T. Wrin, G. Skowron, S. G. Deeks, M. Bates, N. S. Hellmann, and C. J. Petropoulos.** 2002. Hypersusceptibility to non-nucleoside reverse transcriptase inhibitors in HIV-1: clinical, phenotypic and genotypic correlates. AIDS **16:**F41–F47.
49. **Zuber, B., D. Bottiger, R. Benthin, P. T. Haaft, J. Heeney, B. Wahren, and B. Oberg.** 2001. An in vivo model for HIV resistance development. AIDS Res. Hum. Retrovir. **17:**631–635.